Graphical Abstract

Synthesis and DNA binding profile of monomeric, dimeric, and trimeric derivatives of crystal violet

Leave this area blank for abstract info.

Omar Nunez, Bianca Chavez, Ryan Shaktah, Paola Pereda Garcia, and Thomas G. Minehan*

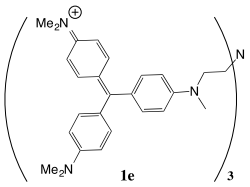

K_a=16.2 x $10^7$$M^{-1}$

Bioorganic Chemistry
journal homepage: www.elsevier.com

Short communication

Synthesis and DNA binding profile of monomeric, dimeric, and trimeric derivatives of crystal violet

Omar Nunez,[a] Bianca Chavez,[a] Ryan Shaktah,[a] Paola Pereda Garcia,[a] and Thomas Minehan[a]*

[a]*Department of Chemistry and Biochemistry, California State University, Northridge, 18111 Nordhoff Street, Northridge, CA 91330, USA*

ARTICLE INFO

Article history:
Received
Received in revised form
Accepted
Available online

Keywords:
Triphenylmethane dyes
Nucleic acids
Major groove
B/B* form DNA
Molecular docking

ABSTRACT

Monomeric, dimeric, and trimeric derivatives of the triphenylmethane dye crystal violet (**1a** – **1f**) have been synthesized for the purpose of evaluating their affinity and sequence selectivity for duplex DNA. Competitive ethidum displacement assays indicate that **1a** – **1f** have apparent association constants for CT DNA in the range of 1.80-16.2 x10^7 M^{-1} and binding site sizes of 10-14 bp. Viscosity experiments performed on ligand **1f** confirmed that these dyes associate with duplex DNA by a non-intercalative mode of binding. Circular dichroism and competition binding studies of the tightest binding ligand **1e** with known major and minor groove binding molecules suggest that these dye derivatives likely occupy the major groove of DNA. Data from the binding of **1e** to polynucleotides indicate close to an order of magnitude preference for associating with AT rich homopolymers over GC rich homopolymers, suggesting a shape-selective match of the sterically bulky ligand with DNA containing a wider major groove.

1. Introduction

The triphenylmethane dyes fuchsin, malachite green, crystal violet, and methyl green are all histochemical stains which are known to bind duplex DNA (Figure 1).[1] Previous studies on the interaction of these compounds with nucleic acids have revealed a non-intercalative mode of association and a preference for binding DNA over RNA.[2] Furthermore, evidence presented by Kim and Norden[3] suggests that methyl green binds to the major groove of DNA. In contrast, the vast majority of nucleic acid-binding small molecules and natural products prefer to occupy the narrower minor groove, where hydrophobic and van der Waals interactions with the walls and floor of the groove are maximized.[4] The notable exceptions to this trend are the pluramycins, aflatoxins, azinomycin, leinamycin, and neocarzinostatin i-gb.[5] Intercalation of a planar delocalized-π system into the backbone of DNA is a consistent binding mode among all of these natural products, and with the exception of the aflatoxins, all of these substances also possess polar major-groove binding moieties. The process of intercalation dramatically alters the structure of duplex DNA far from the drug binding site;[6] the lengthening and rigidification of the double helix is evidenced by viscosity increases of DNA solutions containing added intercalators.[7]

In studies directed toward the development of sequence-specific major-groove binding small molecules,[11] we desired a non-intercalating molecular scaffold that could direct attached moieties into the major groove.

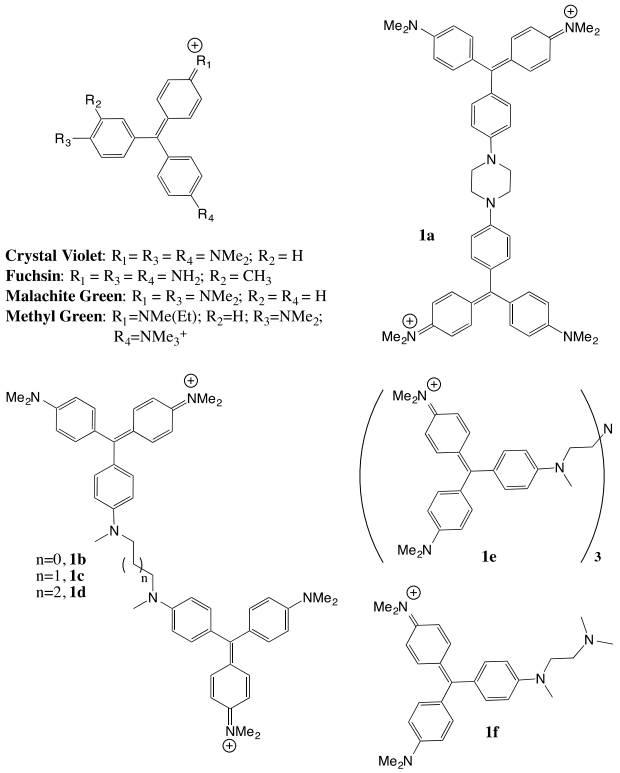

Figure 1. Structures of cationic dyes and synthetic derivatives **1a-1f**.

* Corresponding author. Tel.: +1-818-677-3315; fax: +1-818-677-4068; e-mail: thomas.minehan@csun.edu

As an initial step toward this goal, we wished to study the DNA binding mode and affinity of a series of derivatives (**1a-1f**) of the cationic dye crystal violet (Figure 1),[8] which can be readily prepared by addition of Grignard reagents derived from 4-bromo-*N,N*-dimethylaniline to diverse ethyl 4-*N,N*-dialkylaminobenzoates.[9] DNA binding ligands possessing positively charged residues have a high affinity for duplex nucleic acids due to electrostatically favourable interactions with the negatively charged phosphate backbone and electronegative atoms in the major and minor grooves.[10] Dimeric (**1a-1d**) and trimeric (**1e**) derivatives of crystal violet would thus be expected to bind tightly to duplex DNA, and varying the distances between the dye units with flexible (**1b-1e**) and non-flexible (**1a**) tethers would allow us to probe the optimal distance between charges for DNA association. Monomeric derivative **1f** would allow an assessment the benefits of attaching more than one dye unit to a diamine tether. Finally, the steric bulk of the triphenylmethane moieties was expected to favour ligand binding in major groove of DNA.[3]

2. Results and Discussion

2.1 Chemistry

Reaction of piperazine, *N,N*-dimethylethylenediamine, *N,N*-dimethylpropylenediamine, and *N,N*-dimethylbutylenediamine with ethyl-4-fluoro benzoate (**2**) in DMF in the presence of potassium carbonate (12 h, 150 °C, Scheme 1) gave rise to the corresponding (bis)-aniline derivatives **3a-3d**;[12] treatment of these intermediates with excess (4-(dimethylamino)phenyl) magnesium bromide in THF at 60 °C for two hours,[9] followed by reaction quench with 1N HCl, gave rise to the triphenylmethane derivatives **1a-1d** in 30-46% overall yields after flash chromatography. Treatment of **2** with tris(2-methylaminoethyl)amine in DMF in the presence of potassium carbonate (12 h, 150 °C) gave rise to triester **3e**, which upon exposure to (4-(dimethylamino)phenyl)magnesium bromide in THF at 60 °C for two hours, followed by reaction quench with 1N HCl, provided ligand **1e** in 33% overall yield. Finally, addition of *N, N, N'*-trimethylethylenediamine to **2** under basic conditions furnished **3f**, which reacted with (4-(dimethylamino)phenyl)magnesium bromide in a similar fashion to provide **1f** in 75 % yield after purification.

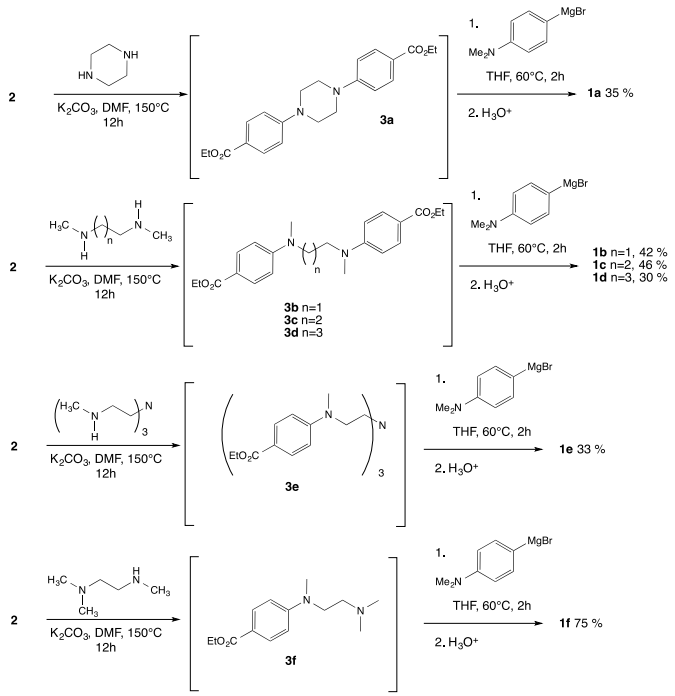

Scheme 1. Synthesis of ligands **1a-f**.

2.2 DNA binding evaluation

To compare the strengths of binding of compounds **1a-1f** to calf thymus (CT) DNA, the competitive ethidium displacement technique was employed to obtain apparent association constants (K_{app})[13] and binding ratios (r_{bd}).[14] In accord with the previous findings of Waring et al. for crystal violet (association constant K_a=1.5 x 10^5 M^{-1}; nucleotides per bound molecule, n=4.5),[2] the sigmoidal binding plots for ligands **1a-1f** revealed at least two distinct complexes with DNA (Figure 2). As seen in Table 1, the tightest binding synthetic ligand was the trimeric derivative **1e** (K_{app}=16.2±3.7 x 10^7 M^{-1}). Interestingly, monomeric dye **1f** and dimeric dyes **1a-1d** all have similar affinities for CT DNA (K_{app}=1.8-4.2 x 10^7 M^{-1}), indicating a strong correlation between the degree of positive charge on the ligand and its tightness of binding (see below).

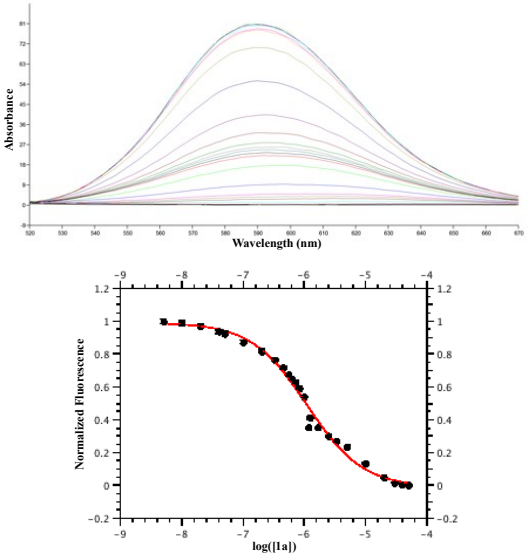

Figure 2. Displacement of ethidium bromide from CT DNA by **1a**.

Crystal violet (CV) has also been shown to significantly increase the stability of CT DNA toward thermal denaturation, raising the melting temperature of native DNA by as much as 19 °C at ~2:1 base pair/ligand ratios.[2] We also performed thermal denaturation studies by monitoring the absorption at 260 nm in the ultraviolet spectrum of CT DNA in the presence and absence of compounds **1a-1f** over the temperature range 25 °C - 90 °C.[15] At CT DNA (bp): ligand ratios of 50:1, strong stabilization of the DNA duplex by the dimeric ligand **1a** (ΔT_M = 10.2 °C) and the trimeric ligand **1e** (ΔT_M = 7.0 °C) was observed, while a relatively minimal effect on the CT DNA T_m value was recorded for the monomeric ligand **1f**. These findings are indicative of the beneficial effect of additional triarylmethane moieties on helix stability, most likely because of the establishment of additional van der Waals interactions between the ligand and DNA.

Table 1. Estimation of CT-DNA apparent association constants (K_{app}), stoichiometry (r_{bd}), and ΔT_M values for ligands **1a-f**.

Ligand	K_{app} (x10^7 M^{-1})[a]	r_{bd}[b]	ΔT_M (°C)[c]
1a	1.80±0.04	11.0	10.2
1b	4.19±0.58	14.1	3.0
1c	2.87±0.35	10.4	4.4
1d	1.87±0.39	11.9	2.5
1e	**16.2±3.7**	**11.0**	**7.0**
1f	2.28±0.06	9.5	0.5

[a] Average K_{app} values obtained by the competitive ethidium displacement method (10 mM Tris-EDTA, pH=5.48), where $K_{app}=K_e$ x C_e/C_{50} and $K_e=2.1 \times 10^6 M^{-1}$.[13] [b] r_{bd} (ratio of CT DNA (bp):ligand) values were determined from the breakpoint of the curve in a plot of Δ

fluorescence vs. CT DNA:ligand ratio, with the data obtained from the competitive ethidium displacement method.[14] [c] T_M values obtained (10 mM phosphate buffer, pH = 7.0) from first derivative analysis ($\Delta A/\Delta T$ vs. ΔT) of the sigmoidal melting curves (A vs. T); $\Delta T_M = T_M$(CT DNA + ligand)-T_M(CT DNA). The ratio of CT DNA: ligand for the thermal denaturation experiments was 50:1.[15] [d] A significant ΔT_M value could not be determined at the CT DNA: ligand ratio of 50:1.

To investigate the importance of electrostatic interactions[10] in the binding of the dye derivatives to DNA, we evaluated the association of both **1c** and **1e** with CT DNA under high- and low-salt conditions using the ethidium displacement assay (See Figure 3 and ESI). For both ligands, increasing NaCl concentrations in the buffer (10 μM CT DNA in 10 mM Tris-EDTA, pH=5.48) from 0.001-0.100 M results in a three-fold drop in the C_{50} value (concentration of ligand required to achieve a 50% decrease in the fluorescence of ethidium). A plot of log(K_{app}) vs. –log(I) for **1c** and **1e** gave a straight line with a slope of ~2.5, indicating the release of 2-3 counterions upon ligand binding (see ESI).[16] These data indicate that the positively charged nitrogen atoms of the dye units are involved in ionic interactions with the phosphate backbone and perhaps also polar hydrogen bonding interactions in the grooves of DNA.

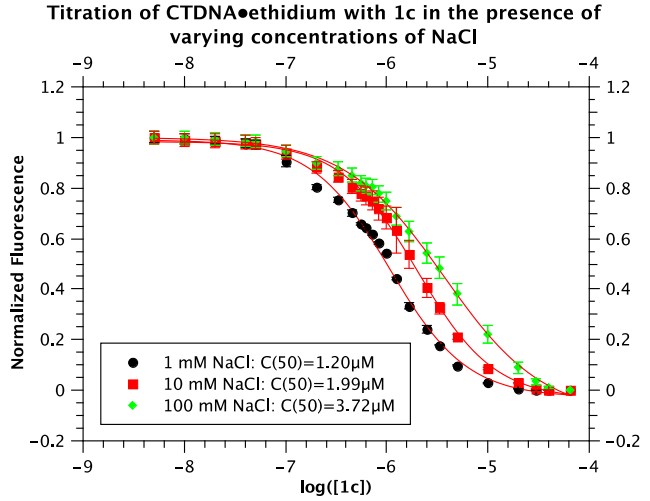

Figure 3. Titration of CT DNA (10 μM) and ethidium (10 μM) and either 1 mM (black circles), 10 mM (red squares), or 100 mM (green diamonds) NaCl with **1c**: 0.005, 0.01, 0.02, 0.04, 0.05, 0.1, 0.2, 0.33, 0.45, 0.56, 0.63, 0.71, 0.83, 1.00, 1.25, 1.67, 2.50, 3.30, 5.0, 10.0, 20.0, 30.0, 40.0, 50.0 μM.

To evaluate the groove occupancy of the dye ligands, we investigated the displacement of ethidium bromide from CT DNA by **1e** in the presence of either the minor groove binding agent netropsin (NP, 10 μM) or the major groove binding agent methyl green (MG, 10 μM).[3] The addition of netropsin actually resulted in a slight *decrease* in the C_{50} value (concentration of **1e** required to achieve a 50% decrease in the fluorescence of ethidium) from 2.00 μM to 1.60 μM (Figure 4). In contrast, the addition of methyl green instead resulted in a pronounced increase in the C_{50} value from 2.00 μM to 6.91 μM, corresponding to an approximately 3.5-fold drop in the binding affinity of **1e** for CT DNA. These data suggest that an important binding site of **1e** is likely the major groove of DNA; subsequent experiments (see below) provided additional evidence supporting major groove occupancy by **1e**.

Next, the binding of **1e** to different DNA polynucleotides was examined using the ethidium displacement assay (Table 2). Compound **1e** bound the homopolymer poly dA•polydT with the highest affinity of all the polymers tested (C_{50}=0.66±0.10 μM), which was more than 2-fold greater affinity than for the binding of **1e** to the alternating polymer poly(dAdT)$_2$ (C_{50}=1.41±0.28 μM), and more than 3-fold greater affinity than for the binding of **1e** to CT DNA (C_{50}=1.99±0.12 μM). In contrast, **1e** bound poly dG•poly dC with almost 8-fold lower affinity (C_{50}=5.02±0.74 μM) than poly dA•polydT. Similarly, the RNA duplex poly A•poly U (C_{50}=4.27±0.10) was bound with 6.5-fold lower affinity than poly dA•poly dT, mirroring the observations of Waring on the weaker binding of CV to RNA.[2] The affinity of **1e** for DNA from *micrococcus luteus* (72% G+C, C_{50}=1.88±0.14 μM) was similar to that for CT DNA; however, lambda phage DNA (C_{50}=2.35±0.18 μM) was bound with a slightly lower affinity than CT DNA. Lambda phage DNA[17] is methylated in the major groove (*N6*-methyl adenine, *C5*-methyl cytosine), and thus the lower binding observed for the association of **1e** with phage DNA is suggestive of major groove binding, since the minor groove binder netropsin binds to lambda phage DNA with a slightly *higher* apparent affinity than to calf thymus DNA (see ref 11). The preference of compound **1e** for binding the homopolymer poly dA•poly dT may reflect a shape complementarity between the sterically bulky dye derivative and the wider major groove of B/B*-form DNA.[24] In contrast, the dye binds more weakly to the narrower major groove of GC-rich DNA and A-form RNA.[25]

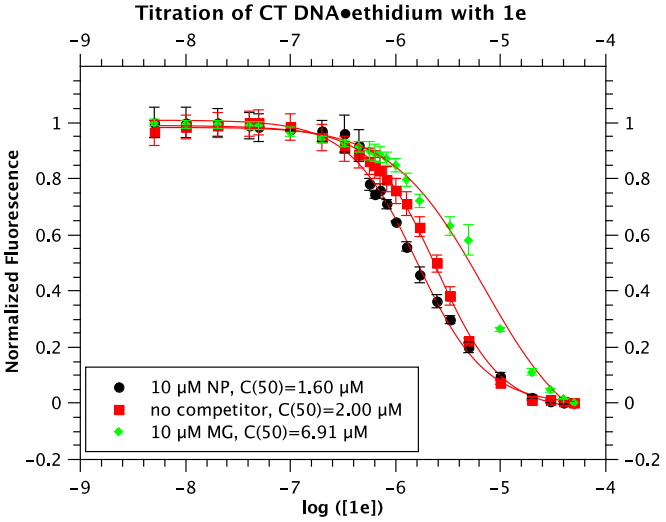

Figure 4. Binding isotherms for the titration of CT DNA (10□□M) and ethidium (10□□M) with 1e (10 mM Tris-EDTA, 10 mM NaCl, pH=5.48) in the absence of competitor (red squares) or in the presence of netropsin (black circles) or methyl green (green diamonds). Black circles: 10 □M netropsin, K_a = 13.1 ± 1.4 x 10^7 M^{-1}; red squares: no competitor, K_a = 10.5 ± 0.6 x 10^7 M^{-1}; green diamonds: 10 □M methyl green, K_a = 3.04 ± 0.46 x 10^7 M^{-1}.

Table 2. Evaluation of the binding of **1e** to different DNA polynucleotides by ethidium displacement assay.

Nucleic acid	C_{50}(μM)
polydG•polydC	5.02±0.74
m. luteus	1.88±0.14
calf thymus	1.99±0.12
poly(dA•dT)$_2$	1.41±0.28
lambda phage	2.35±0.18
polyA•polyU	4.27±0.10
polydA•polydT	**0.66±0.10**

To further probe the mode of binding of **1e** to duplex DNA, we monitored the UV absorbance of **1e** at 542 nm upon titration with CT-DNA (see ESI). A distinct hypochromic shift along with a slight hypsochromic (blue) shift to 530 nm was observed, findings which are not consistent with an intercalative mode of binding.[18] Indeed, viscosity studies performed on ligand **1f**

(Figure 5) indicated that increasing concentrations of the ligand in the presence of CT-DNA resulted in a slight *decrease* in solution viscosity; in contrast, increasing concentrations of the intercalator ethidium bromide showed a distinct increase in solution viscosity, while increasing amounts of the minor groove binder netropsin resulted in negligible changes in viscosity.[6,7] These results are fully consistent with those obtained by Waring on crystal violet and are indicative of a non-intercalative mode of DNA binding for this class of dyes.[2]

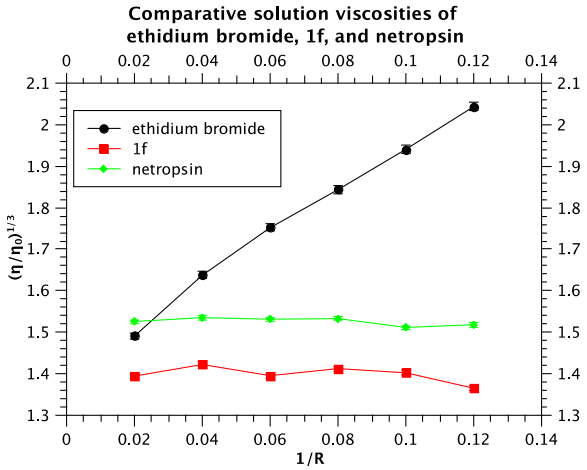

Figure 5. Effect of increasing amounts of **1f** (■), ethidium bromide (●), and netropsin (♦) on the relative viscosity of CT-DNA. *R*= [DNA(bp)]/[ligand]; **1f** (■): [CT-DNA] = 300 μM, [**1f**]: 1, 2, 4, 10, 18, and 26 μM; ethidium bromide (●): [CT-DNA] = 300 μM, [ethidium bromide]= 4, 26, 70, 113, 160, and 200 μM; netropsin (♦): [CT-DNA] = 300 μM, [netropsin]= 4, 26, 70, 113, 160, and 200 μM.

CD spectra of CT DNA recorded in the 215-330 nm region in the presence of increasing concentrations of **1e** revealed only minor perturbations of both the helicity band at 240 nm and base-stacking band at 280 nm at low **1e**:DNA ratios, followed by an increase in the base stacking band and a red shift in both bands at higher ligand concentrations (Figure 6). These findings, which again are inconsistent with intercalative binding,[19] suggest that the triphenylmethane dyes do not dramatically alter the structure of DNA at low ligand:DNA ratios. In addition, a strong negative induced CD (ICD) band appeared at ~310 nm at higher **1e** concentrations, an observation consistent with major-groove binding.[20]

2.2 Molecular docking studies

Finally, molecular docking studies of ligand **1e**[21] with the Dickerson-Drew dodecamer (5'-CGCGAATTCGCG-3') (PDB 436D)[23] were performed using Autodock vina.[22] The lowest energy binding mode shows the trimeric dye bound in the major groove of B-form DNA with two triphenylmethane units spanning the double helix near the end of the dodecamer to engage in ionic contacts with the phosphate backbone. In addition, nitrogen atoms in the linker moiety appear to be involved in hydrogen-bonding contacts with polar hydrogen atoms displayed on the floor of the major groove in the central AT-rich region of the helix (Figure 7). Though the DNA search space included both major and minor grooves, none of the computed binding modes showed the ligand associating with the minor groove.

3. Conclusions

We have prepared a series of monomeric (**1f**), dimeric (**1a-1d**), and trimeric (**1e**) derivatives of the dye crystal violet that show sub-micromolar binding affinities for duplex DNA. Salt studies performed on ligands **1c** and **1e** have demonstrated a strong ionic component to the DNA binding affinity of these ligands; furthermore, viscosity experiments performed on ligand **1f** indicate that these molecules do not intercalate the backbone of DNA. Competition binding assays performed with **1e** and known major- and minor-groove binding agents, as well as ICD bands observed during CD titrations of CT DNA with **1e**, strongly suggest that these molecules preferentially associate with the major groove of DNA. Binding experiments with polynucleotides suggest a shape-selective binding of the sterically bulky dye derivative **1e** to AT-rich B/B*-form DNA, which contains a wider major groove.

These studies indicate that positively charged triarylmethanes are non-intercalating DNA-binding moieties that may serve to direct appended groups to the major groove, the principal site of association for regulatory proteins. Further experiments to characterize the binding (by ITC) of **1a-1f** to oligonucleotides of defined sequence are underway and will be reported in due course

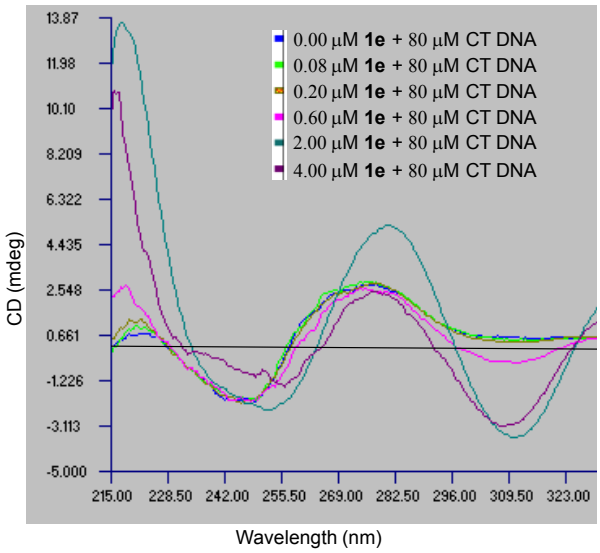

Figure 6. The 220-310 nm region of the CD spectrum of solutions of CT DNA (80 □M) in the absence (black line) and presence of various concentrations of **1e**: blue line 0.0 □M **1e**, light green line, 0.08□□M **1e**; orange line, 0.20 □M **1e**; light red line, 0.06 □M **1e**; dark green line 2.00 □M **1e**; purple line: 4.00 □M **1e**.

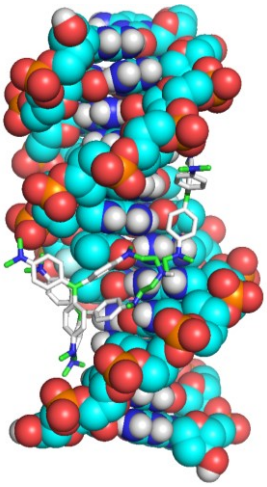

Figure 7. Model for the binding of ligand **1e** in the major groove of the Drew-Dickerson dodecamer (5'-CGCGAATTCGCG-3').

4. Experimental part

4.1 General

Distilled water was used in all of the experiments. Reagents and solvents were used as supplied, with the following exceptions: CH_2Cl_2 was distilled from CaH_2; Et_2O was distilled from $LiAlH_4$; THF was distilled from sodium benzophenone ketyl; toluene and benzene were dried over 4Å molecular sieves. Organic extracts were dried over Na_2SO_4, filtered, and concentrated using a rotary evaporator at aspirator pressure (20-30 mmHg). Chromatography refers to flash chromatography and was carried out on SiO_2 (silica gel 60, 230-400 mesh). ^1H and ^{13}C NMR spectra were measured in $CDCl_3$ at 400 MHz and 100 MHz, respectively, using Me_4Si as internal standard. Chemical shifts are reported in parts per million (ppm) downfield (□) from Me_4Si. For ^1H NMR, multiplicity (s=singlet, d=doublet, dd=doublet of doublets, t=triplet, q=quartet, br=broad, m=multiplet) and coupling constants (in Hz) were reported whenever possible. ^{13}C spectra were recorded with complete proton decoupling.

4.1.1 General procedure for the synthesis of **1a-1f**

1a-1d: The diamine (1.5 mmol) was dissolved in DMF (1.5 mL), and potassium carbonate (420 mg, 3 mmol) and ethyl-4-fluorobenzoate (510 mg, 3 mmol) was added. The reaction was heated under reflux for 8 hours. Upon cooling to room temperature, water (4.0 mL) was added and the mixture was extracted with ethyl acetate (10 mL). The phases were separated and the organic layer was further extracted with brine (2 x 10 mL), dried over anhydrous sodium sulfate, filtered, and concentrated *in vacuo*. The crude material was subjected to rapid silica gel chromatography (5:1→1:1 hexanes:ethyl acetate) to provide the intermediate diester. In a 25 mL round-bottom flask was placed magnesium metal (381 mg, 15.7 mmol), which was flame-dried under vacuum to remove trace amounts of moisture; THF (1.4 mL) was then added. Separately, 4-bromo-*N,N*-dimethylaniline (2.57 g, 12.9 mmol) was dissolved in THF (1.4 mL) and a chip of iodine was added. The solution of the bromide was added dropwise to the magnesium metal with gentle heating until reaction took place; then the remainder of the bromide solution was added and the mixture was heated to 50 °C for two hours. Upon cooling to room temperature, the intermediate diester (545 mg, 1.42 mmol) in THF (1.4 mL) was added dropwise and the mixture was allowed to stir at room temperature overnight under argon. The mixture was then carefully quenched with 1M HCl (5 mL) and dichloromethane (20 mL) and water 10 mL) were added. The phases were separated and the aqueous layer was further extracted with CH_2Cl_2 (4 x 10 mL). The combined organics were dried over anhydrous sodium sulfate, filtered, and concentrated *in vacuo*. The crude residue was then purified by flash chromatography to yield compounds **1a-1d**.

1e: Following the general procedure for the synthesis of **1a-1d**, tris[2-(methylamino)ethyl]amine (1.0 g, 5.3 mmol), ethyl-4-fluorobenzoate (2.67 g, 15.8 mmol), and 4-bromo-*N,N*-dimethylaniline (10.7 g, 54 mmol) were combined to give **1e** after purification by flash chromatography.

1f: Following the general procedure for the synthesis of **1a-1d**, *N,N,N'*-trimethylethylene-diamine (176.8 mg, 1.73 mmol), ethyl-4-fluorobenzoate (510 mg, 2.6 mmol), and 4-bromo-*N,N*-dimethylaniline (1.60 g, 8.0 mmol) were combined to give **1f** after purification by flash chromatography.

4.1.2 $(CV)_2$-piperazine **1a**

Following the general procedure, piperazine (128 mg, 1.5 mmol), ethyl-4-fluorobenzoate (510 mg, 3 mmol), and 4-bromo-*N,N*-dimethylaniline (2.57 g, 12.9 mmol) gave after flash chromatography ($CHCl_3$/MeOH 20:1-2:1, 1 drop conc. NH_4OH) **1a** (430 mg, 0.53 mmol, 35%). R_f = 0.5 (3:1 $CHCl_3$:MeOH, 1 drop conc. NH_4OH. **^1H NMR** (400 MHz, $CDCl_3$) δ 7.36 (d, *J*=8.8 Hz, 12H); 7.19 (d, *J*=8.1 Hz, 4H); 6.88 (d, *J*=9.0 Hz, 8H); 4.12 (s, 8H); 3.29 (s, 24H). **^{13}C NMR** (100 MHz, $CDCl_3$) δ 178.2, 155.7, 154.8, 139.9, 139.6, 127.7, 126.6, 113.3, 112.5, 45.8, 40.6. **HRMS**–ESI (m/z): calculated for $C_{50}H_{56}N_6$: 370.2283 (M^{2+}) found 370.2281 (M^{2+}).

4.1.3 $(CV)_2$-ethane **1b**

Following the general procedure, 1,2-dimethylethylenediamine (132 mg, 1.5 mmol), ethyl-4-fluorobenzoate (510 mg, 3 mmol), and 4-bromo-*N,N*-dimethylaniline (3.99 g, 20.0 mmol) gave after flash chromatography ($CHCl_3$/MeOH 20:1-2:1, 1 drop conc. NH_4OH) **1b** (512 mg, 0.63 mmol, 42 %). R_f = 0.5 (3:1 $CHCl_3$:MeOH, 1 drop conc. NH_4OH). **^1H NMR** (400 MHz, $CDCl_3$) δ 7.35 (d, *J*=9.0 Hz, 12H); 7.00 (d, *J*=8.0 Hz, 4H); 6.88 (d, *J*=9.1 Hz, 8H); 4.14 (s, 4H); 3.33 (s, 6H); 3.28 (s, 24H). **^{13}C NMR** (100 MHz, $CDCl_3$) δ 177.9, 155.6, 154.7, 139.8, 139.7, 127.1, 126.6, 112.6, 112.5, 50.5, 40.7, 40.1. **HRMS**–ESI (m/z): calculated for $C_{50}H_{58}N_6$: 371.2362 (M^{2+}), found 371.2381 (M^{2+}).

4.1.4 $(CV)_2$-propane **1c**

Following the general procedure, 1,3-dimethylpropylenediamine (87 mg, 0.85 mmol), ethyl-4-fluorobenzoate (289 mg, 1.7 mmol), and 4-bromo-*N,N*-dimethylaniline (1.18 g, 5.9 mmol) gave after flash chromatography ($CHCl_3$/MeOH 20:1-2:1, 1 drop conc. NH_4OH) **1c** (322 mg, 0.39 mmol, 46 %). R_f = 0.5 (4:1 $CHCl_3$:MeOH, 1 drop conc. NH_4OH). **^1H NMR** (400 MHz, $CDCl_3$) δ 7.28 (m, 12H); 7.1 (m, 4H); 6.82 (m, 8H); 3.94 (m, 4H); 3.33 (s, 3H); 3.32 (s, 3H); 3.24 (s, 24H); 2.16 (s, 2H). **^{13}C NMR** (100 MHz, $CDCl_3$) δ 166.9, 152.1, 131.3, 117.6, 110.6, 60.1, 49.9, 38.4, 30.9, 24.4, 14.4. **HRMS**–ESI (m/z): calculated for $C_{51}H_{60}N_6$: 378.2439 (M^{2+}), found 378.2388 (M^{2+}).

4.1.5 $(CV)_2$-butane **1d**

Following the general procedure, 1,4-dimethylbutylenediamine (150.8 mg, 1.3 mmol), ethyl-4-fluorobenzoate (442 mg, 2.6 mmol), and 4-bromo-*N,N*-dimethylaniline (2.62 g, 13.1 mmol) gave after flash chromatography ($CHCl_3$/MeOH 20:1-2:1, 1 drop conc. NH_4OH) **1d** (328 mg, 0.39 mmol, 30 %) R_f = 0.5 (4:1 $CHCl_3$:MeOH, 1 drop conc. NH_4OH). **^1H NMR** (400 MHz, $CDCl_3$) δ 7.31 (m, 12H); 6.92 (d, *J*=8.7 Hz, 4H); 6.83 (d, *J*=8.6 Hz, 8H); 3.70 (m, 4H); 3.26 (s, 6H); 3.23 (s, 24H); 1.85 (m, 4H). **^{13}C NMR** (100 MHz, $CDCl_3$) δ 177.8, 155.4, 155.1, 140.1, 139.5, 126.6, 112.7, 112.3, 52.6, 40.4, 39.2, 24.7. **HRMS**–ESI (m/z): calculated for $C_{52}H_{62}N_6$: 385.2518 (M^{2+}), found 385.2548 (M^{2+}).

4.1.6 $(CV\text{-}CH_2CH_2)_3N$ **1e**

Following the general procedure, tris[2-(methylamino)-ethyl]amine (1.0 g, 5.3 mmol), ethyl-4-fluorobenzoate (2.67 g, 15.8 mmol), and 4-bromo-*N,N*-dimethylaniline (10.7 g, 54 mmol) gave after flash chromatography ($CHCl_3$/MeOH 20:1-2:1, 1 drop conc. NH_4OH) **1e** (2.2 g, 1.74 mmol, 33 %). R_f = 0.5 (4:1 $CHCl_3$:MeOH, 1 drop conc. NH_4OH). **^1H NMR** (400 MHz, $CDCl_3$) δ 7.26 (m, 16H); 7.17 (m, 3 H); 6.95 (m, 5H); 6.83 (d, *J*=9.2 Hz, 12H); 3.82-2.97 (m, 12H); 3.33 (s, 9 H); 3.24, (s, 36H). **^{13}C NMR** (100 MHz, $CDCl_3$) δ 155.5, 139.8, 139.6, 126.5, 112.6, 112.4, 52.1, 40.6, 40.0. **HRMS**–ESI (m/z): calculated for $C_{52}H_{62}N_6$: 389.9195 (M^{3+}), found 389.9205 (M^{3+}).

4.1.7 CV-$CH_2CH_2N(CH_3)_2$ **1f**

Following the general procedure, *N,N,N'*-trimethylethylene-diamine (176.8 mg, 1.73 mmol), ethyl-4-fluorobenzoate (510 mg, 2.6 mmol), and 4-bromo-*N,N*-dimethylaniline (1.60 g, 8.0 mmol) gave after flash chromatography ($CHCl_3$/MeOH 20:1-2:1, 1 drop conc. NH_4OH) **1f** (602 mg, 1.30 mmol, 75 %) R_f = 0.5 (4:1 $CHCl_3$:MeOH, 1 drop conc. NH_4OH). **^{1}H NMR** (400 MHz, $CDCl_3$) δ 7.24 (d, *J*=9.2 Hz, 6H); 6.82 (d, *J*= 9.2 Hz, 2H); 6.78 (d, *J*=9.2 Hz, 4H); 3.69 (t, *J*=7.2 Hz, 2H); 3.19 (s, 15H); 2.68 (t, *J*=6.9 Hz, 2H); 2.34 (s, 6H).**^{13}C NMR** (100 MHz, $CDCl_3$) δ 177.9, 155.5, 154.6, 139.6, 126.5, 112.3, 55.5, 50.4, 45.3, 40.6, 39.4. **HRMS**–ESI (m/z): calculated for $C_{28}H_{38}N_4$: 430.3096, found 430.3112 $(M+H)^+$.

4.2 Competitive ethidium bromide displacement

Constant concentrations of CT-DNA, polydG•polydC, poly dA•poly dT, poly(dA-dT)•poly(dA-dT), polyA•polyU, *M. Luteus* DNA, or Lambda phage DNA (10 μM) and EtBr (10 μM) were titrated with increasing concentrations of the ligands (from 1 mM and 100 μM stock solutions), in the presence or absence of fixed concentrations of NaCl or the competitors methyl green or netropsin. The maximum emission wavelength was 490 nm when the excitation wavelength was 520 nm. Fluorescence titrations were recorded from 520 nm to 692 nm after an equilibration period of 3 min. Ex Slit (nm) = 10.0; Em Slit (nm) = 10.0; Scan Speed (nm/min) = 200.

4.3 Thermal denaturation studies

UV thermal denaturation samples (2 mL) were prepared by mixing CT-DNA in 100 mM NaCl and 10 mM Tris-EDTA buffer (pH 5.38) in 1 cm path length quartz cuvettes. The DNA to ligand ratio was 50:1. Absorbance readings were taken at 260 nm for temperatures ranging from 25℃ to 95℃. Temperature was increased gradually with a speed of 1°C/min with an absorbance reading every 2°C. First derivative plots were used to determine the T_M value.

4.4 Viscosity studies

Viscosity experiments were performed with an Ostwald viscometer in a constant water bath at 23.0 ± 1°C. Solutions of constant DNA concentrations and varying ligand concentrations in Tris-EDTA buffer were incubated for 30 minutes. A digital stopwatch was used to record the flow time. The relative viscosity was calculated as from the following equation:

$$\eta = t\text{-}t_o/t_o$$

where t_0 and t are the flow time in the absence and presence of the ligand. η is the viscosity in the presence of the ligand and η_0 is the viscosity in the absence of the ligand. The data were graphed as $(\eta/\eta_0)^{1/3}$ vs. [ligand]/[DNA].

4.5 Circular dichroism studies

Small aliquots (0.6-5.0 μL) of a concentrated **1e** solution (1 mM) were added to a solution (2 mL, 100 mM KCl, 10 mM SC, 0.5 mM EDTA, pH 6.8) of CT-DNA (80 μM/bp), inverted twice, and incubated for 5 min at 20 °C. The CD spectra were then recorded as an average of three scans from 220 to 330 nm and data recorded in 0.1 nm increments.

4.6 Molecular docking studies

Compound **1e** was minimized using Spartan 14 for Macintosh.[21] Molecular docking studies were performed with **1e** and the Dickerson-Drew dodecamer (5'-CGCGAATTCGCG-3') (PDB 436D)[23] using Autodock vina.[22] The search space included both major and minor grooves.

Acknowledgments

This paper is dedicated to Professor Yoshito Kishi on the occasion of his 80th birthday. We thank the National Science Foundation (CHE-1508070) and the donors of the American Chemical Society Petroleum Research fund (53693-URI) for their generous support of our research program. BC thanks the NIH MARC program (GM008395) for support. We thank Milena Balazy, Steven Ayoub, and Lizette Aburto for initial fluorescence studies on ligands **1a-1d** and the melting temperature determinations in Table 1. We thank Alejandra Fausto for assistance with fluorescence-based assays.

References and notes

1 W. Muller and F. Gautier, *Eur. J. Biochem.* 1975, **54**, 385.
2 (a) L. P. G. Wakelin, A. Adams, C. Hunter, M. J. Waring *Biochemistry* **1981**, *20*, 5779. (b) Y. Chen, J. Wang, Y. Zhang, L. Xi, T. Gao, B. Wang, R. Pei *Photochem. Photobiol. Sci.* 2018, ahead of print.
3 S. K. Kim and B. Norden, *FEBS Letters* 1993, **315**, 61.
4 W. C. Tse and D. L. Boger, *Chem. Biol.* 2004, **11**, 1607.
5 P. L. Hamilton and D. P. Arya, *Nat. Prod. Rep.* 2012, **29**, 134.
6 D. Suh and J. B. Chaires *Bioorg. Med. Chem.* 1995, **3**, 723.
7 P. C. Dedon In *Curr. Protoc. Nucleic Acid. Chem.* 2000, New York: John Wiley and Sons, 8.1.1.
8 T. Gessner and U. Mayer In *Ullmann's Encyclopedia of Industrial Chemistry* 2000, Weinheim: Wiley-VCH, 6.1.1.
9 D. F. Taber, R. P. Meagley, D. J. Supplee, *J. Chem. Ed.* 1996, **73**, 259.
10 V. K. Misra and B. Honig, *Proc. Natl. Acad. Sci.* 1995, **92**, 4691.
11 M. Balazy, A. Fausto, C. Voskanian, B. Chavez, H. Panesar, T. G. Minehan, *Org. Biomol Chem.* 2017, **15**, 4522.
12 A. Mayence, J. J. Vanden Eynde, F. M. Krogstad, D. J. Krogstad, M. T. Cushion, T. L. Huang, *J. Med. Chem* 2004, **47**, 2700.
13 A. R. Morgan, J. S. Lee, D. E. Pulleyblank, N. L. Murray, D. H. Evans, *Nucleic Acids Res.* 1979, **7**, 547.
14 S. Kumar, L. Xue, D. P. Arya, *J. Am. Chem. Soc.* 2011, **133**, 7361.
15 W. D. Wilson, F. A. Tanious, M. Fernandez-Saiz, C.T. Rigl, *Methods in Mol. Biol. Drug-DNA Interact. Protoc.* 1997, **90**, 219.
16 J. Nygren, N. Svanvik, M. Kubista *Biopolymers* 1998, **46**, 39.

17 From *E. coli* host strain W3110: A. M. Desimone and J. D. Laney *Mol. Cell. Biol.* 2010, **30**, 3342.

18 L. Perez-Flores, A. J. Ruiz-Chica, J. G. Delcros, F. Sanchez-Jimenez, F. J, Ramirez, *J. Mol. Struct.* 2005, **744-747**, 699.

19 N. C. Garbett, P. A. Ragazzon, J. B. Chaires *Nature Protocols*, 2007, **2**, 3166.

20 (a) K. Triantafillidi, K. Karidi, J. Malina, A. Garoufis *Dalton Trans.* 2009, 6403. (b) M. J. Hannon, V. Moreno, M. J. Prieto, E. Moldrheim, E. Sletten, I. Meistermann, C. J. Isaac, K. J. Sanders and A. Rodger, *Angew. Chem., Int. Ed*., 2001, **40**, 880.

21 Minimized using Spartan 14 for Macintosh (Wavefunction, Inc., Irvine, CA).

22 (a) O. Trott, A. J. Olson, *J. Comput. Chem.* 2010, **31**, 455. (b) The search space included both major and minor grooves as well as the phosphate backbone.

23 V. Tereshko, G. Minasov, M. Egli, *J. Am. Chem. Soc* 1999, **121**, 470.

24 B^* form DNA refers to AT rich DNA sequences that contain long A tracts that lead to an unusually narrow minor groove: N. V. Hud, J. Plavec, *Biopolymers* 2003, **69**, 144.

25 For similar observations by Arya on neomycin-neomycin dimer, see reference 14.

Supplementary Material

Supplementary data (synthetic procedures, spectroscopic data and ^{1}H and ^{13}C NMR spectra) associated with this article can be found, in the online version, at.